

Studies on the role of co-oxidant and surfactant in interfacial polymerisation of polyaniline nanofibers and its nonlinear optical limiting applications

Divya P. R.^{1*}, P. M. Sabura Begum¹, Rani Joseph², Indu Sebastian³

¹Department of Applied Chemistry, Cochin University of Science and Technology, Cochin 682022, India

²Department of Polymer Science and Rubber Technology, Cochin University of Science and Technology, Cochin 682 022, India

³International School of Photonics, Cochin University of Science and Technology, Cochin 682022, India

*Corresponding author. Tel: (+91) 9495979376; E-mail: divu10@gmail.com

Received: 11 November 2015, Revised: 11 February 2016 and Accepted: 01 June 2016

ABSTRACT

Herein, we have prepared Polyaniline (PANI) nanofibers by interfacial polymerization in the presence of co-oxidant and surfactant. The additives are found to have a profound impact on the polymers morphology and improved room temperature conductivity. It was found that PANI nanofibers prepared in the presence of aqueous sodium hypochlorite solution (NaOCl) and cetyl trimethyl ammonium bromide (CTAB) were of shorter diameter (30 nm) and high conductivity (6.59Scm^{-1}) than those formed in the absence of those chemicals. The diameter of the fibers was intricately tuned by changing the ratio of NaOCl to aniline. The effect of co-oxidant and surfactant concentration in the nanofibers has been investigated with the help of SEM, IR, XRD, UV and conductivity studies. A comparative investigation with other surfactant sodium dodecyl sulphate (SDS) has been done and the variations in diameter were noted. We also studied the third-order optical nonlinearity and optical limiting properties of polyaniline nanofibers using a single-beam z-scan technique. The experiments were performed with a Nd-YAG laser at wavelength of 532 nm. The mechanism behind nonlinear absorption could be predicted as two photon absorption. The results show that the polyaniline nanofibers have useful applications in futuristic nonlinear optics. Copyright © 2016 VBRI Press.

Keywords: Polyaniline; nanofibers; interfacial polymerisation; nonlinear optical properties.

Introduction

Intrinsically conducting polymers are attractive materials, as they exhibit opto-electrical properties of a metal or a semiconductor. Additionally, they are light weight, flexible, inexpensive and easy to synthesis [1]. Conducting polymers are composed of pi-conjugated polymer chains and counter ions produced by a doping process [2]. Polyaniline (PANI) has been intensively studied in the field of conducting polymers due to its unique chemical structure and properties, such as extended conjugation through a heteroatom, multiple oxidation states. Also the electrical and optical properties of polyaniline can be controlled by a simple and reversible acid–base doping–dedoping process [3, 4]. Nanostructures of polyaniline are of great current interest in view of the fact that such materials possess the advantages of both low-dimensional organic conductors and high surface area materials. These low-dimensional polyaniline nanostructures including nanoparticles, nanorods, nanofibers, nanowires, nanotubes, nanoflakes, nanoplates, and nanodisks, having physical and chemical properties differing from their bulk counterparts play integral part for applications such as polymeric conducting

molecular wires [5], chemical sensors [6-8], biosensors [9] and electromagnetic shielding devices [10].

Researchers have identified that well-defined and ultimately noticed nanostructured morphology for polyaniline is the nanofiber. It was reported that polyaniline tends to intrinsically form nanofibrous structures at the initial period of the polymerization process, and then acted as scaffolds for the secondary overgrowth of irregularly-shaped polyaniline [11-13]. Films containing polyaniline nanofibers can be made by using electrospinning [14] or electrochemical methods to control the polymerization rate [15-17]. Other synthetic approaches to the chemical synthesis of polyaniline nanofibers include nanofiber seeding [18], oligomer-assisted polymerization [19], surfactant-assisted polymerization [20] and non-template polymerization [21]. PANI nanofibers synthesized by Huang *et al.* by a novel interfacial polymerization method include an immiscible organic/ aqueous biphasic system [22, 23]. Khalid *et al.* developed a synthesis based on the interfacial polymerization method where sulfonated porphyrin acts as an in situ dopant [24]. They reported that the electrostatic and hydrophobic interactions between the water dispersible porphyrin complex and the dimer cation-

radical surfactant are responsible for the formation of nanofibers. Few reports have appeared in the literature examining the role of acidic medium and aniline to oxidant ratio in interfacial phenomena on conducting polymer morphology. Recently Li *et al.* prepared three different nanostructured polyanilines by interfacial polymerization using different inorganic acids including HCl, H₂SO₄, and HNO₃ as aqueous reaction media [25]. It is found that the reaction medium plays a vital role in deciding the morphology, conductivity, crystalline property of the products.

Among π -conjugated organic polymers, PANI has been enormously investigated to determine its capability for nonlinear optical applications as they possess third-order nonlinear optical properties [26]. Since they retain prominent nonlinearity and ultra-fast response time, PANI have received remarkable attention in applications like photonic switching devices, opto-electronic materials for light emitting diodes, solar cells, and xerographic photoreceptors [27-30]. Optical power limiters are widely used in order to control the intensity of light that are in demand for the development of optical technology. PANI also used in Optical limiting devices those strongly attenuate optical beams at high intensities while exhibiting higher transmittance at low intensities. Such devices are applicable for the protection of the human eye and optical sensors from intense laser beams [31-34]. In recent, S Pramodini *et al.* present the a lower limiting threshold and clamping level for the conducting polymers poly (aniline-co-o-anisidine) and poly (aniline-co-pyrrole) by employing the z-scan technique using a He-Ne laser operating in continuous wave mode at 633 nm[35].

In this study, an interfacial polymerization method with the co-use of co-oxidant (NaOCl), surfactants is proposed for the synthesis of polyaniline nanofibers in which aniline is chemically and oxidatively polymerized to polyaniline at the interface of two immiscible liquids. The influence of the additives on the morphology and related properties of polyaniline nanofibers was investigated. Also the nonlinear optical properties and strong optical limiting power of polyaniline nanofibers with nanosecond Nd: YAG laser pulses at 532 nm were discussed.

Experimental

Materials

Aniline (99.5 %), ammonium peroxy disulfate (98 %), D(+)-10-camphor sulfonic acid (CSA)(99 %), cetyl trimethyl ammonium bromide (CTAB), aqueous sodium hypochlorite (4 % by wt) solution (NaOCl), carbon tetrachloride (CCl₄), sodium dodecyl sulphate (SDS) are used. These chemicals were purchased from Spectrochem Pvt. Ltd. Mumbai, India. Aniline was distilled and stored at 4 °C prior to usage. All other chemicals were used as received without further purification. Deionized water was used throughout all the processes.

Synthesis of polyaniline nanofibers

The polymerization of aniline was carried out in the interface of two immiscible solvents (water/CCl₄). In a typical synthesis, 0.32 M distilled aniline was dissolved in

the CCl₄ (this has density higher than water) and 0.007 M CTAB was added and stirred for 30 minutes at 0-5 °C. In another beaker, added 0.08 M APS into 1 M camphor sulfonic acid (CSA) and allowed to stir for 30 minutes using magnetic stirrer. And again stirred with 3 % aqueous sodium hypochlorite solution (NaOCl) and placed for one hour at 0 - 5°C. The above two phases were gently transferred to a reaction vial generating an interface between the two layers. Green polyaniline nanofibers were formed at the interface. As the reaction proceeded, it got migrated gradually into the aqueous phase until the whole aqueous phase is filled homogeneously with dark green PANI. The mixed solution was placed room temperature for 24 hours. After polymerization, the entire water phase was then collected, and the by-products were removed by filtration and washing several times with water, followed by drying in an oven at 80 °C overnight yielding PANI nanofibers in the form of green powder. A part of the nanofibers was dedoped by treatment with 0.1 M NH₄OH aqueous solution and was labeled PANI-EB. Different types of PANI nanofibers were prepared by changing the volume % of NaOCl solution from 1 %, 2 %, 3 % and 4 % of NaOCl solution and labeled PANI-1, PANI-2, and PANI-3 and PANI-4 respectively. As a comparison, PANI nanofibers were synthesized in the absence of NaOCl designated as PANI-CTAB and in the absence of both surfactant and NaOCl designated as PANI-CSA via the similar procedure mentioned above. The whole experiment was also done by changing surfactant to sodium dodecyl sulfate (SDS). By changing the volume % of NaOCl solution, SDS-1 and SDS-2 (with 2 % NaOCl and 4 % NaOCl respectively) were prepared.

Characterizations of polyaniline nanofibers

Scanning electron microscopy (SEM) observations of all the powdered samples were examined using a JEOL Model JSM 6390 LV scanning electron microscope. Qualitative elemental analysis is performed with Energy Dispersive Spectrometer JEOL Model JED – 2300. The TEM images were taken on a transmission electron microscopy (Jeol/JEM 2100, with an accelerating voltage of 200 kV, point resolution: 0.23 nm). Fourier transform infrared spectra (FTIR) were recorded on a Jasco FT/IR-4100 instrument using KBr pressed pellets. Ultraviolet-visible (UV-vis) diffuse reflectance spectroscopy (DRS) of PANI nanofibers was recorded on a UV/VIS/NIR spectrophotometer Model: Varian, Cary 5000. X-ray diffraction (XRD) patterns were obtained using a Bruker AXS D8 Advance X-ray powder diffractometer equipped with Cu K α radiation. The samples were scanned in the range of 2 - 25° 2 θ at increments of 0.020° at a wavelength of 1.541 Å operating at 40 KV and 35 mA. DC electrical conductivity measurements were done by a standard four-probe electrode using a Keithley 2400 source-measure unit in dry air at ambient Temperature. Chemically prepared polymer samples in the powder form are pelletised to form pellets of about 1 cm diameter with thickness less than 1mm. The nonlinear optical characterization of the samples was carried out using the Z-scan technique at 532 nm. The samples to be investigated were translated through the focal point of a lens of focal length 20 cm. The beam waist radius ω_0 was estimated to be 35.4 μ m. The Rayleigh length

$Z_0 = \pi \omega_0^2 / \lambda$ was calculated to be 7.4 mm. The samples were taken in 1mm cuvette which is much lesser than Z_0 ; therefore, the essential prerequisite for z-scan experiment is satisfied.

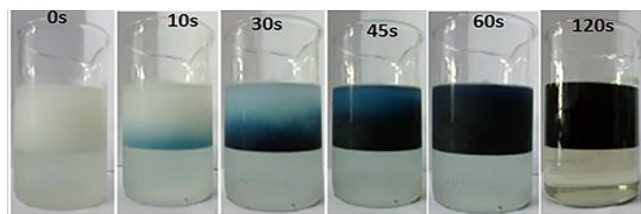


Fig. 1. Digital photographs of the interfacial polymerization of aniline at the interface of camphor sulphonic acid / carbon tetrachloride. The reaction times are marked on the glassware. The top phase is 1M CSA, APS and NaOCl, and the bottom phase is aniline and CTAB dissolved in carbon tetrachloride.

Results and discussion

Fig. 1 illustrated the process of interfacial polymerization of polyaniline nanofibers. The top phase of beaker is aqueous phase (CSA) and the bottom phase is organic phase (CCl_4). It can be clearly seen that the green polyaniline nanofibers formed at the interface and the rate of polymerisation is very high in initial stage. In an immiscible organic (mixture of aniline and organic solvent CCl_4)/aqueous (CSA and APS solution) biphasic system, the oxidation of aniline occurs at the interface of the two liquids and polyaniline nanofibers form at the interface within a few minutes. Then nanofibers migrate into the aqueous phase since it is hydrophilic in nature. The nanofibers stay away from the reactive interface so they are not subject to further secondary growth [36].

The SEM images of PANI nanofibers are shown in **Fig. 2**. To get the optimal conditions for the synthesis of polyaniline nanofibers, we investigated the influence of surfactant and co-oxidant in the reaction. When the reaction was carried out without surfactant and co-oxidant (PANI-CSA), fibers approximately 75 nm in diameter were produced (**Fig. 2a**). However, when the reaction was conducted in the presence of CTAB (PANI-CTAB), the resulting fibers have slightly larger diameter (82 nm), as shown in **Fig. 2b**.

We also investigated the effect of NaOCl concentration on the morphology of the polymerization product, and found that as the hypochlorite concentration was increased from 1 % to 3 %, the diameter of nanofibers decreases (~66 nm with 1% NaOCl, ~57 nm with 2 % NaOCl to ~30 nm with 3% NaOCl) as shown in **Fig. 2(c), (d) & (e)**. On further increase in the concentration of hypochlorite to 4 % agglomeration of nanofibers, the nanofiber morphology begins to disappear. Thus, 3 % concentration of hypochlorite is favorable for the synthesis of small diameter fibers. The diameter of the fibers could be directly controlled by the appropriate selection of hypochlorite concentration. Here the co-oxidant NaOCl helps to increase the initial rate of polymerisation while surfactant CTAB facilitates the interaction between aqueous phase and organic phase in the reaction mixture. Also organic dopant camphor sulphonic acid has good interfacial packing properties which favors nanofibrillar morphology and better water solubility [37].

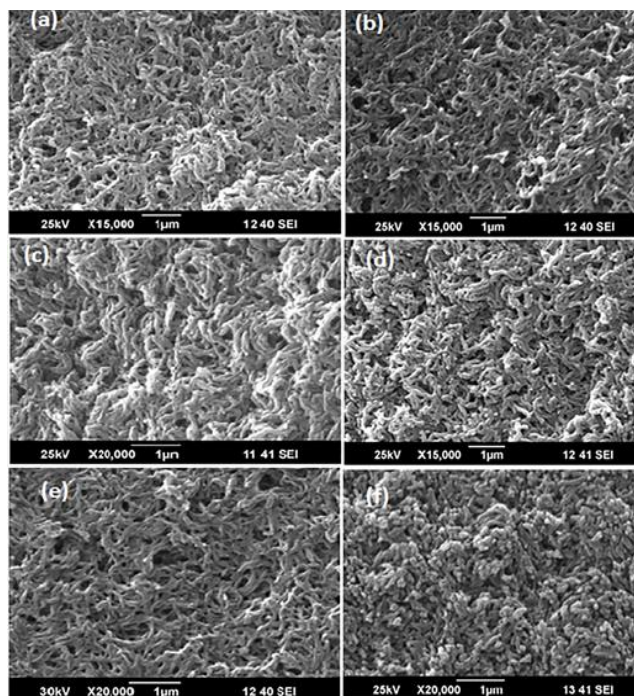


Fig. 2. SEM images of (a) PANI-CSA, (b) PANI-CTAB, (c) PANI-1, (d) PANI-2, (e) PANI-3 and (f) PANI-4.

Fig. 3(a-c) shows the SEM images of polyaniline samples obtained from addition of another surfactant sodium dodecyl sulfate (SDS). We observed that in this case, polyaniline nanofibers obtained have larger diameters above 100 nm. Upon the addition of hypochlorite, the diameter of nanofibers further increased (~106 nm with 0 % NaOCl, ~160 nm with 2% NaOCl to ~192 nm with 4% NaOCl) as seen in **Fig 3(b, c)**. The differences in the diameter of the prepared polyaniline nanofibers with CTAB and SDS may be explained by the variation of the local environment formed by different surfactants.

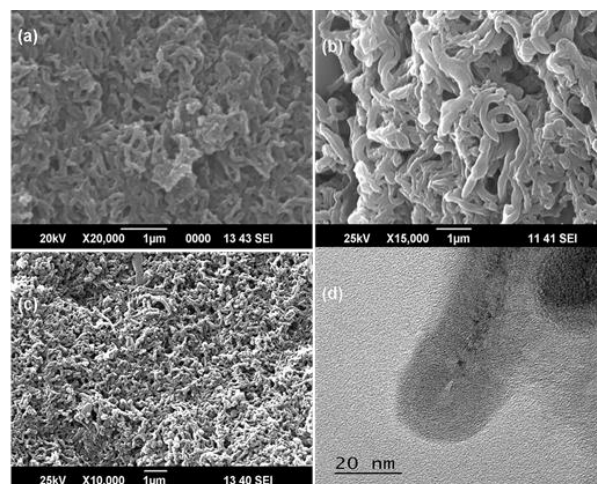


Fig. 3. SEM images of (a) PANI-SDS, (b) PANI-SDS-1, (c) PANI-SDS-2 & (d) TEM image of polyaniline nanofiber PANI-3.

TEM image of PANI-3 shown in **Fig. 3(d)** indicated that the nanofibers have uniform diameter approximately 30 nm and nanofibers produced are longer and entangled. This morphology of polyaniline can be related to the fast rate of

polymerization in initial stage, and under this condition, polyaniline nanofibers can be easily synthesized by homogeneous nucleation process and thus suppressing the secondary overgrowth [38].

Table 1. Conductivity and diameter of the samples under different reaction conditions.

Sample	Surfactant used	Amount of NaOCl used	Conductivity (Scm ⁻¹)	Diameter (nm)
PANI-CSA	-----	-----	3.99 ± 0.17	75 ± 3
PANI-CTAB	CTAB	-----	2.82 ± 0.24	82 ± 5
PANI-1	CTAB	1%	1.94 ± 0.09	66 ± 4
PANI-2	CTAB	2%	3.72 ± 0.18	57 ± 3
PANI-3	CTAB	3%	6.59 ± 0.15	30 ± 4
PANI-4	CTAB	4%	4.18 ± 0.22	52 ± 6
PANI-SDS	SDS	-----	1.98 ± 0.32	106 ± 10
PANI-SDS-1	SDS	2%	4.23 ± 0.25	160 ± 7
PANI-SDS-2	SDS	4%	7.56 ± 0.30	192 ± 9

The room-temperature conductivities of polyaniline nanofibers were obtained using the standard four-probe method. The electrical conductivity of PANI-CSA was determined to be 3.99 Scm⁻¹. As shown in **Table 1**, the conductivity increased with the addition of hypochlorite solution, and PANI-3 which have smaller diameter giving the highest conductivity (6.59 Scm⁻¹) among the CTAB based samples.

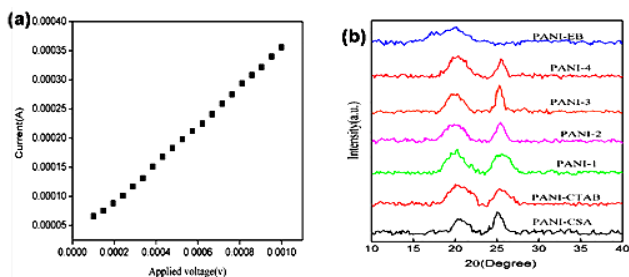


Fig. 4. (a) I–V characteristics of PANI-3 measured in air at room temperature (b) XRD scattering pattern of PANI fibers.

The conductivity of PANI depends on the degree of doping, oxidation state, particle morphology, crystallinity, inter- or intrachain interactions, molecular weight, etc. We can see that the fiber diameter has a significant effect on the conductivity of PANI. A decrease in diameter value can lead to more effective doping; higher degree of crystallinity, and higher conductivity, however, too small particle size will produce some lattice defect, more localized electron and lower conductivity [39]. This suggests that the conductivity increases with the addition of hypochlorite is due to the increase of efficiency of charge transfer along the polyaniline backbone. The current (I)–voltage (V) characteristics of the PANI nanofibers (PANI-3) shown in **Fig. 4(a)** The I–V curves indicated ohmic behavior; that is, current changed linearly with voltage. In the case of SDS based samples, the dc electrical conductivity increased upon the addition of hypochlorite solution. Since CTAB is a cationic surfactant and SDS is an anion surfactant, they form positively charged interfaces and negatively charged interfaces in solutions respectively. The local environment formed by SDS micelles that can provide a higher charge density than that of CTAB which promote the formation of conducting PANI [40]. Also

cationic dodecyl sulfonate which derives from SDS can act as dopant while CTAB cannot supply such counterions for doping PANI. This lead to the better conductivity of polyaniline nanofibers formed with the assistance of SDS and NaOCl.

Careful analysis of XRD pattern of PANI shown in **Fig. 4(b)** suggests that it exhibits a semi crystalline behavior. The doped PANI nanofibers exhibit two broad peaks at 2θ angles around 20° and 25°, correspond to the (100) and (110) crystal planes which indicates PANI contains some crystalline domains [41,42]. The peaks at 2θ=20° and 2θ=25° in doped PANI are due to the periodicity parallel and perpendicular to the polymer chain respectively [43]. In the XRD pattern of dedoped form PANI-EB, we observe a broad hump, having a maximum around 20° indicates amorphous nature and its intrinsic crystallinity is due to the presence of a polar nitrogen atom in the main backbone chain [44].

Table 2. EDX analysis data for PANI nanofibers.

Sample	Elements (atom %)				
	C	N	O	S	Cl
PANI-CSA	88.03	1.10	5.26	5.61	---
PANI-CTAB	87.34	0.97	5.91	5.78	---
PANI nanofibers(PANI-3)	88.68	1.03	5.14	4.55	0.60
PANI-SDS	86.81	0.80	7.45	4.94	---

While in the doped forms the presence of polarons or charge defects enhances its crystallinity. PANI-3 shows much sharper peaks compared to others which indicates higher the degree of crystallinity of the sample. The higher degree of crystallinity or more ordered structural pattern in PANI causes intra-molecular mobility of charged species along the chain and to some extent intermolecular hopping because of better and closer packing. Hence, the increase in the crystallinity is expected to increase the conductivity [45]. This is also in agreement with the results obtained from conductivity measurements. The energy dispersive x-ray analysis gives both qualitative and quantitative information about the element composition of polyaniline nanofibers. **Table 2** represents presence of carbon, oxygen, nitrogen, sulphur and chlorine in the polyaniline nanofibers detected from EDX spectrum shown in **Fig. 5(a)**. **Fig. 5(b)** represents the FT-IR spectra of synthesized polyaniline nanofibers and the peak locations related to the corresponding chemical bonds are in good agreement with those reported in the literature. The characteristic vibration bands of polyaniline are located at 1481 and 1557 cm⁻¹, can be assigned to the stretching vibration of quinoid ring and benzenoid ring, respectively. The peaks at 1,299 cm⁻¹ correspond to the C–N stretching vibration of secondary aromatic amine [46]. The inplane bending of C–H is reflected in the 1,124 cm⁻¹ peak. The peak at 800 cm⁻¹ is attributed to the out-of-plane bending of C–H bond [47].

The Optical band gaps of polyaniline nano fibers were determined by the diffuse reflectance measurements. Thus obtained, reflectivity spectra can be converted to equivalent absorption spectra using the Kubelka–Munk (KM) function. The KM function at any wavelength is given as,

$$F(R_{\infty}) = \frac{(1 - R_{\infty})^2}{2R_{\infty}} \quad (1)$$

Here, $F(R_{\infty})$ is the remission or Kubelka–Munk function, R_{∞} is the reflectance of the sample relative to the reference material, α is the absorption coefficient and s in the scattering coefficient. Typically, the scattering coefficient is only weakly dependent on energy. Therefore, $F(R_{\infty})$ can be assumed to be proportional to the absorption spectrum [48].

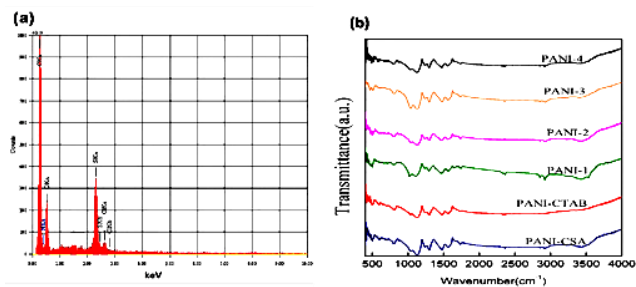


Fig. 5. (a) EDX spectra of PANI-3 (b) FTIR spectra of PANI nanofibers synthesizer in different reaction conditions.

The photon absorption in many amorphous materials is found to obey the Tauc relation [49], which is of the form,

$$ahv = B(hv - Eg)^n \quad (2)$$

where, α is the absorption coefficient, $h\nu$ is the photon energy, B is the band gap tailing parameter, Eg is a characteristic energy which is termed as optical band gap and n is the transition probability index, which has discrete values $n = 1/2, 3/2, 2$ and 3 for direct allowed, direct forbidden, indirect allowed and indirect forbidden electronic transitions, respectively [50].

$F(R_{\infty})$ is determined from Eq.1 and plot of $(F(R_{\infty})/h\nu)^2$ (index $n = 1/2$) versus $h\nu$ shows a linear portion at the absorption edge which confirms the existence of direct allowed band transition in polyaniline nanofibers. Extrapolating of linear dependence of the relation to abscissa yields the corresponding direct allowed band gap. The values of the optical direct transition energies obtained are 3.13 eV, 3.21 eV and 3.05 eV for PANI-CSA, PANI-CTAB and PANI-3 respectively. In order to determine the indirect transition energy gap, plots of $((F(R_{\infty})/h\nu)^{1/2})$ as a function of photon energy versus $h\nu$ was plotted. The value of the optical indirect transition energies was found to be 2.38 eV, 2.45 eV and 2.15 eV for PANI-CSA, PANI-CTAB and PANI-3 respectively. The lower band gap for the PANI-3 indicates relatively easier polaron/ bipolaron transition occurring in it which is responsible for its higher conductivity [51].

The nonlinear optical characterization of the polyaniline nanofiber was carried out using the Z-scan technique at 532 nm at a typical influence of 181 MW/cm². The open-aperture Z-scan curve exhibits a normalized transmittance valley, indicating reverse saturable absorption in the polyaniline nanofiber. The data were analysed using the procedure described by Bahae *et al.* [52].

The nonlinear absorption coefficient is obtained by fitting the experimental z-scan plot to:

$$T(z,s=1) = \frac{1}{\sqrt{\pi q_0(z,0)}} \int_{-\infty}^{\infty} \ln[1 + q_0(z,0) e^{-\tau^2}] d\tau, \quad (3)$$

where,

$$q_0(z,0) = \frac{\beta I_0 L_{eff}}{(1 + z^2/z_0^2)} \quad (4)$$

Here, I_0 is the laser intensity in the focal plane, β is the nonlinear optical absorption coefficient, L_{eff} is the effective thickness with linear absorption coefficient α .

L_{eff} is given by,

$$L_{eff} = (1 - e^{-\alpha l})/\alpha \quad (5)$$

The open aperture z-scan measurement for polyaniline nanofibers is depicted in **Fig. 6(a)**.

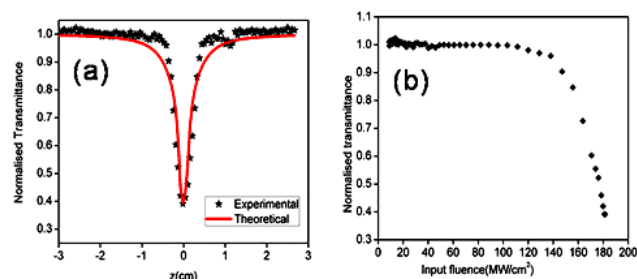


Fig. 6. (a) Normalized transmittance as a function of the position in the open aperture scheme and (b) Optical limiting response of polyaniline nanofiber at 532nm at an input power density of 181 MW/cm².

The fits of Eq. (3) to experimental data are shown as solid red curves. From the fit, we can confirm that the basic mechanism involved in the nonlinear absorption of polyaniline nanofiber is two photon absorption processes. When the samples are away from the focus, the light intensity is low. It is clear that, polyaniline nanofibers exhibit a clear decrease in transmission with increasing input laser intensity as the sample is translated towards focus, indicating the occurrence of reverse saturable absorption process (RSA) [53]. The nonlinear absorption coefficient (β) numerically evaluated from the above fits is 92.6 cm/GW. Reverse saturable absorption has been found to occur in centro-symmetric structural organic materials and especially in pi-conjugated materials like conducting polymers. The extensive pi-electron delocalization present in polyaniline nanofibers causes polarization in the material which assists the ultrafast nonlinear optical response. RSA occurs when the molecules present in ground state and excited states can absorb the incident photons of same wavelengths and the absorption of excited states must be larger than that of the ground states. RSA also known as positive nonlinear absorption type of behavior results due to any of the nonlinear mechanisms such as two-photon absorption (TPA), excited free carrier absorption (ESA) or with the combination of the processes [54].

The optical limiting performance of polyaniline nanofiber was analyzed at an input laser intensity of 181 MW cm⁻²

without aperture under Nd-YAG Laser (532 nm) illumination. **Fig. 6(b)**. Depicts the characteristic optical limiting curves i.e. input intensity versus normalized transmittance.

A salient criterion in the optical limiting process is the limiting threshold (onset optical limiting) which gives the corresponding input fluence value at which the deviation from linearity in the normalized transmittance is observed [55]. The limiting threshold value obtained from **Fig. 6b** is 135.63 MW/cm². Since polyaniline is energy absorbing type of optical limiter, the major nonlinear optical mechanisms responsible for optical limiting are RSA and ESA arises from an effective two photon absorption which leading to nonlinear absorption in organic molecules [56].

Conclusion

The interfacial polymerization of aniline in the presence of co-oxidant and surfactant can produce polyaniline nanofibers with enhanced properties. Co-oxidant and surfactant can influence the polymer morphology and room temperature conductivity. SEM, TEM images and four probe conductivity measurements revealed that nanofibers formed by the co-use of surfactant CTAB and 3% NaOCl solution gave shorter diameter (30 nm) fiber with better conductivity (6.59 S/cm) than other nanofibers. The formation of conducting emeraldine salt phase of the polymer was confirmed by the FT-IR spectroscopy and is supported by X-ray diffraction analysis. The improved conducting nature was further supported by the UV-DRS measurements. This research therefore provides a simple, reliable, and scalable route for synthesizing PANI nanofibers with better morphology and good conductivity. The polymer samples exhibited third-order nonlinear optical properties with a reverse saturable absorption process and strong optical power limiting properties under the experimental conditions. Thus the investigated polymers emerge as a potential candidate for optical limiting devices under continuous wave laser at the experimental wavelength.

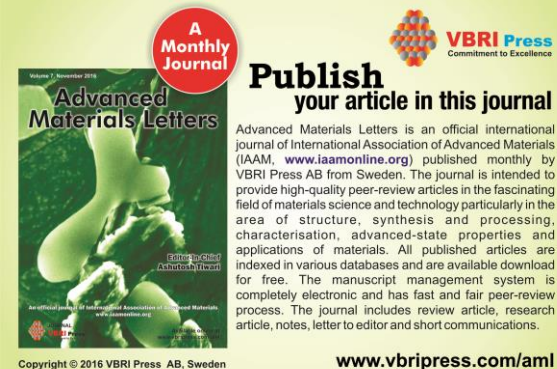
Acknowledgements

The authors gratefully thank Sophisticated Analytical Instruments Facility (SAIF), STIC, Cochin University of Science and Technology (CUSAT) for the characterization facilities. They also wish to acknowledge CSIR research fellowship for financial support through research work.

References

- Deore, B. A.; Freund, M. S.; *Macromolecules*, **2009**, *42*, 164.
DOI: [10.1021/ma8020344](https://doi.org/10.1021/ma8020344)
- Skotheim, A.; Elsenbaumer, R. L.; Reynolds, J. R. (Eds.); *Handbook of Conducting Polymers* 2nd ed.; Marcel Dekker: New York, **1998**.
- Negi, Y. S.; Adhyapak, P. V.; *J. Macromol. Sci. polymer reviews C*, **2002**, *42*, 35.
DOI: [10.1081/MC-120003094](https://doi.org/10.1081/MC-120003094)
- Kang, E. T.; Neoh, K. G.; Tan, K. L.; *Prog. Polym. Sci.*, **1998**, *23*, 211.
DOI: [10.1016/S0079-6700\(97\)00030-0](https://doi.org/10.1016/S0079-6700(97)00030-0)
- Cattena, C. J.; Bustos-Marín, R. A.; Pastawski, H. M.; *PHYSICAL REVIEW B*, **2010**, *82*, 144201.
DOI: [10.1103/PhysRevB.82.144201](https://doi.org/10.1103/PhysRevB.82.144201)
- Virji, S.; Huang, J.; Kaner, R. B.; Weiller, B. H.; *Nano Lett.*, **2004**, *4*, 491.
DOI: [10.1021/nl035122e](https://doi.org/10.1021/nl035122e)
- Zeng, F. W.; Liu, X. X.; Diamond, D.; Lau, K.T.; *Sensors and Actuators B*, **2010**, *143*, 530.
DOI: [10.1016/j.snb.2009.09.050](https://doi.org/10.1016/j.snb.2009.09.050)
- Bai, S.; Sun, C.; Wan, P.; Wang, C.; Luo, R.; Li, Y.; Liu, J.; Sun, X.; *Small*, **2015**, *11*, 306.
DOI: [10.1002/smll.201401865](https://doi.org/10.1002/smll.201401865)
- Dhand, C.; Das, M.; Datta, M.; Malhotra, B. D.; *Biosensors and Bioelectronics*, **2011**, *26*, 2811.
DOI: [10.1016/j.bios.2010.10.017](https://doi.org/10.1016/j.bios.2010.10.017)
- Joseph, N.; Varghese, J.; Sebastian, M. T.; *RSC Adv.*, **2015**, *5*, 20459.
DOI: [10.1039/C5RA02113H](https://doi.org/10.1039/C5RA02113H)
- Stejskal, J.; Sapurina, I.; Trchova, M.; *Prog. Polym. Sci.*, **2010**, *35*, 1420.
DOI: [10.1016/j.progpolymsci.2010.07.006](https://doi.org/10.1016/j.progpolymsci.2010.07.006)
- Huang, J.; Kaner, R.; *Chem. Commun.*, **2006**, *4*, 367.
DOI: [10.1039/B510956F](https://doi.org/10.1039/B510956F)
- Zhang, L.; Wan, M.; *Adv. Funct. Mater.*, **2003**, *13*, 815.
DOI: [10.1002/adfm.200304458](https://doi.org/10.1002/adfm.200304458)
- MacDiarmid, A. G.; Jones, W. E.; Norris, I. D.; Gao, J.; Johnson, A. T.; Pinto, N. J.; Hone, J.; Han, B.; Ko, F. K.; Okuzaki, H.; Llaguno, M.; *Synth. Met.*, **2001**, *119*, 27.
DOI: [10.1016/S0379-6779\(00\)00597-X](https://doi.org/10.1016/S0379-6779(00)00597-X)
- Choi, S. J.; Park, S. M.; *J. Electrochem. Soc.*, **2002**, *149*, E26.
DOI: [10.1149/1.1432675](https://doi.org/10.1149/1.1432675)
- Liu, J.; Lin, Y. H.; Liang, L.; Voigt, J. A.; Huber, D. L.; Tian, Z. R.; Coker, E.; Mckenzie, B.; Mcdermott, M. J.; *Chem. Eur. J.*, **2003**, *9*, 604.
DOI: [10.1002/chem.200390064](https://doi.org/10.1002/chem.200390064)
- Liang, L.; Liu, J.; Windisch, C. F.; Exarhos, G. J.; Lin, Y. H.; *Angew. Chem.*, **2002**, *114*, 3817.
DOI: [10.1002/1521-3757\(20021004\)114:19<3817::AID-ANGE3817>3.0.CO;2-F](https://doi.org/10.1002/1521-3757(20021004)114:19<3817::AID-ANGE3817>3.0.CO;2-F)
- Zhang, X.; Goux, W. J.; Manohar, S. K.; *J. Am. Chem. Soc.*, **2004**, *126*, 4502.
DOI: [10.1021/ja031867a](https://doi.org/10.1021/ja031867a)
- Li, W.; Wang, H. L.; *J. Am. Chem. Soc.*, **2004**, *126*, 2278.
DOI: [10.1021/ja039672q](https://doi.org/10.1021/ja039672q)
- Zhang, X.; Manohar, S. K.; *Chem. Commun.*, **2004**, 2360.
DOI: [10.1039/B409309G](https://doi.org/10.1039/B409309G)
- Huang, K.; Wan, M.; *Synth. Met.*, **2003**, *135*, 173.
DOI: [10.1016/S0379-6779\(02\)00560-X](https://doi.org/10.1016/S0379-6779(02)00560-X)
- Huang, J.; Virji, S.; Weiller, B. H.; Kaner, R. B.; *J. Am. Chem. Soc.*, **2003**, *125*, 314.
DOI: [10.1021/ja028371y](https://doi.org/10.1021/ja028371y)
- Huang, J.; Kaner, R. B.; *J. Am. Chem. Soc.*, **2004**, *126*, 851.
DOI: [10.1021/ja0371754](https://doi.org/10.1021/ja0371754)
- Khalid, M.; Acuna, J. J. S.; Tumelero, M. A.; Fischer, J. A.; Zoldan, V. C.; Pasa, A. A.; *J. Mater. Chem.*, **2012**, *22*, 11340.
DOI: [10.1039/C2JM31116J](https://doi.org/10.1039/C2JM31116J)
- Li, T.; Qin, Z.; Liang, B.; Tian, F.; Zhao, J.; Liu, N.; Zhu, M.; *Electrochimica Acta*, **2015**, *177*, 343.
DOI: [10.1016/j.electacta.2015.03.169](https://doi.org/10.1016/j.electacta.2015.03.169)
- Sezer, A.; Gurudas, U.; Collins, B.; Mckinlay, A.; Bubb, D. M.; *Chemical Physics Letters*, **2009**, *477*, 164.
DOI: [10.1016/j.cplett.2009.06.070](https://doi.org/10.1016/j.cplett.2009.06.070)
- Marder, S. R.; Sohn, J. E.; Stucky, G. D. (eds.); *Materials for Nonlinear Optics: Chemical Perspectives*; American Chemical Society: Washington, **1991**.
- Gustafsson, G.; Cao, Y.; Treacy, G. M.; Klavetter, F.; Colaneri, N.; Heeger, A. J.; *Nature*, **1992**, *357*, 477.
DOI: [10.1038/357477a0](https://doi.org/10.1038/357477a0)
- Antoniadis, H.; Hsieh, B. R.; Abkowitz, M. A.; Jenekhe, S. A.; Stolka, M.; *Synthetic Metals*, **1994**, *62*, 265.
DOI: [10.1016/0379-6779\(94\)90215-1](https://doi.org/10.1016/0379-6779(94)90215-1)
- Osaheni, J. A.; Jenekhe, S. A.; Perlstein, J.; *Applied Physics Letters*, **1994**, *64*, 3112.
DOI: [10.1063/1.111364](https://doi.org/10.1063/1.111364)
- Tong, R.; Wu, H. X.; Li, B.; Zhua, R.; Youa, G.; Qiana, S.; Lin, Y.; Cai, R.; *Physica B*, **2005**, *366*, 192.
DOI: [10.1016/j.physb.2005.05.026](https://doi.org/10.1016/j.physb.2005.05.026)
- He, G. S.; Gen, C.; Xu, G. C.; Prasad, P. N.; Reinhardt, B. A.; Bhatt, J. C.; Dillard, A. G.; *Opt. Lett.*, **1995**, *20*, 435.
DOI: [10.1364/OL.20.000435](https://doi.org/10.1364/OL.20.000435)
- Ji, C. L.; Chuan, K. W.; Faris, G.; *Phys. Rev. A*, **2007**, *76*, 053804.
DOI: [10.1103/PhysRevA.76.053804](https://doi.org/10.1103/PhysRevA.76.053804)
- Sunita, S.; Devendra, M.; Ghoshal, S. K.; *Opt. Commun.*, **2008**, *281*, 2923.

- DOI: [10.1016/j.optcom.2008.01.010](https://doi.org/10.1016/j.optcom.2008.01.010)
35. Pramodini, S.; Sudhakar, Y. N.; SelvaKumar, M.; Poornesh, P.; *Laser Phys.*, **2014**, *24*, 045408.
DOI: [10.1088/1054-660X/24/4/045408](https://doi.org/10.1088/1054-660X/24/4/045408)
36. Huang, J. X.; Kaner, R. B.; *Angew. Chem. Int. Ed.*, **2004**, *43*, 5817.
DOI: [10.1002/anie.200460616](https://doi.org/10.1002/anie.200460616)
37. Zhang, X.; Chan-Yu-King, R.; Jose, A.; Manohar, S. K.; *Synthetic Metals*, **2004**, *145*, 23.
DOI: [10.1016/j.synthmet.2004.03.012](https://doi.org/10.1016/j.synthmet.2004.03.012)
38. Tran, H. D.; Norris, L.; D'Arcy, J. M.; Tsang, H.; Wang, Y.; Mattes, B. R.; Kaner, R. B.; *Macromol.*, **2008**, *41*, 7405.
DOI: [10.1021/ma800122d](https://doi.org/10.1021/ma800122d)
39. Xia, H.; Wang, Q.; *Journal of Nanoparticle Research*, **2001**, *3*, 401.
DOI: [10.1023/A:1012564814745](https://doi.org/10.1023/A:1012564814745)
40. Hu, X.; Shu, X. S.; Li, X. W.; Liu, S. G.; Zhang, Y. Y.; Zou G. L.; *Enzyme and Microbial Technology*, **2006**, *38*, 675.
DOI: [10.1016/j.enzmictec.2005.08.006](https://doi.org/10.1016/j.enzmictec.2005.08.006)
41. Pouget, J. P.; Jozefowicz, M. E.; Epstein, A. J.; Tang, X.; MacDiarmid, A. G.; *Macromolecules*, **1991**, *24*, 779.
DOI: [10.1021/ma00003a022](https://doi.org/10.1021/ma00003a022)
42. Pan, W.; Yang, S. L.; Li, G.; Jiang, J. M.; *Eur Polym J.*, **2005**, *41*, 2127.
DOI: [10.1016/j.eurpolymj.2005.04.003](https://doi.org/10.1016/j.eurpolymj.2005.04.003)
43. Li, J.; Tang, X.; Li, H.; Yan, Y.; Zhang, Q.; *Synth. Met.*, **2010**, *160*, 1153.
DOI: [10.1016/j.synthmet.2010.03.001](https://doi.org/10.1016/j.synthmet.2010.03.001)
44. Luzny, W.; Sniechowski, M.; Laska, J.; *Synth. Met.*, **2002**, *126*, 27.
DOI: [10.1016/S0379-6779\(01\)00477-5](https://doi.org/10.1016/S0379-6779(01)00477-5)
45. Bhadra, S.; Chattopadhyay, S.; Singha, N. K.; Khastgir, D.; *Journal of Applied Polymer Science*, **2008**, *108*, 57.
DOI: [10.1002/app.26926](https://doi.org/10.1002/app.26926)
46. Trchova, M.; Sedenkova, I.; Stejskal, J.; *Synth. Met.*, **2005**, *154*, 1.
DOI: [10.1016/j.synthmet.2005.07.001](https://doi.org/10.1016/j.synthmet.2005.07.001)
47. Li, H. L.; Wang, J. X.; Chu, Q. X.; Wang, Z.; Zhang, F. B.; Wang, S. C.; *J. Power Sources*, **2009**, *190*, 578.
DOI: [10.1016/j.jpowsour.2009.01.052](https://doi.org/10.1016/j.jpowsour.2009.01.052)
48. Barton, D. G.; Shtein, M.; Wilson, R. D.; Soled, S. J.; Iglesia, E.; *J. Phys., Chem. B*, **1999**, *103*, 630.
DOI: [10.1021/jp983555d](https://doi.org/10.1021/jp983555d)
49. Yang, M.; Cao, K.; Sui, L.; Ying, Q.; Zhu, J.; Waas, A.; Arruda, E. M.; Kieffer, J.; Thouless, M. D.; Kotov, N. A.; *ACS Nano.*, **2011**, *5*, 6945.
DOI: [10.1021/nn2014003](https://doi.org/10.1021/nn2014003)
50. Tseng, R. J.; Huang, J.; Ouyang, J.; Kaner, R. B.; Yang, Y.; *Nano Lett.*, **2005**, *5*, 1077.
DOI: [10.1021/nl050587l](https://doi.org/10.1021/nl050587l)
51. Kondawar, S. B.; Pethe, S. M.; *Adv. Mat. Lett.*, **2014**, *5*, 414.
DOI: [10.5185/amlett.2014.amwc.1039](https://doi.org/10.5185/amlett.2014.amwc.1039)
52. Sheik-Bahae, M.; Said, A. A.; Wei, T. H.; Hagan, D. J.; Van Stryland, E. W.; *IEEE J. Quantum Electron.*, **1990**, *26*, 760.
DOI: [10.1109/3.53394](https://doi.org/10.1109/3.53394)
53. Nagaraja, K. K.; Pramodini, S.; Santhoshkumar, A.; Nagaraja, H. S.; Poornesh, P.; Kekuda, D.; *Optical Materials*, **2013**, *35*, 431.
DOI: [10.1016/j.optmat.2012.09.028](https://doi.org/10.1016/j.optmat.2012.09.028)
54. Frobel, P. G. L.; Suresh, S. R.; Mayadevi, S.; Sreeja, S.; Mukherjee, C.; Muneera, C. I.; *Materials Chemistry and Physics*, **2011**, *129*, 981.
DOI: [10.1016/j.matchemphys.2011.05.045](https://doi.org/10.1016/j.matchemphys.2011.05.045)
55. Sebastian, I.; Divya, S.; Nampoore, V. P. N.; Radhakrishnan, P.; Thomas, S.; *Appl. Phys. Lett.*, **2013**, *102*, 031115.
DOI: [10.1063/1.4789436](https://doi.org/10.1063/1.4789436)
56. Tutt, L.W.; Boggess, T.F.; *Prog. Quant. Elecrr.*, **1993**, *17*, 299.
DOI: [10.1016/0079-6727\(93\)90004-S](https://doi.org/10.1016/0079-6727(93)90004-S)



A Monthly Journal

Publish your article in this journal

Advanced Materials Letters is an official international journal of International Association of Advanced Materials (IAAM, www.iaamonline.org) published monthly by VBRI Press AB from Sweden. The journal is intended to provide high-quality peer-review articles in the fascinating field of materials science and technology particularly in the area of structure, synthesis and processing, characterisation, advanced-state properties and applications of materials. All published articles are indexed in various databases and are available download for free. The manuscript management system is completely electronic and has fast and fair peer-review process. The journal includes review article, research article, notes, letter to editor and short communications.

www.vbripress.com/aml

Copyright © 2016 VBRI Press AB, Sweden

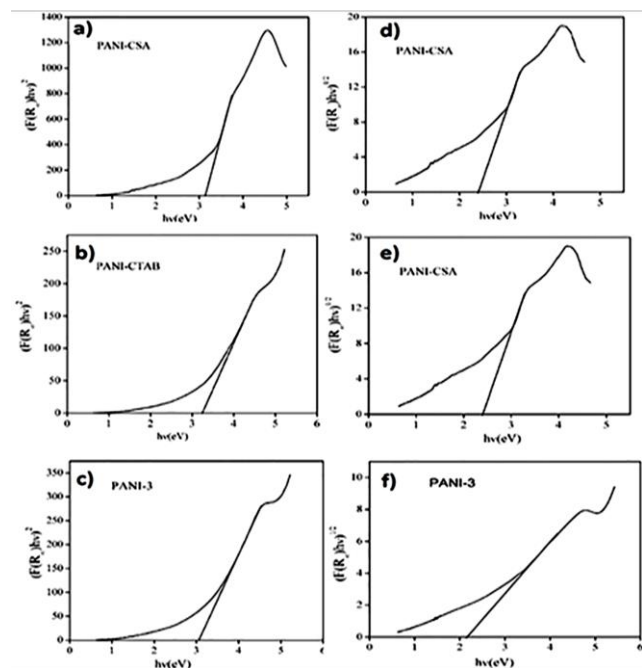
Supporting Information

Fig. Determination of direct band gap energy for PANI nanofibers (a) PANI-CSA, (b) PANI-CTAB, (c) PANI-3 and indirect band gap for PANI (d) PANI-CSA, (e) PANI-CTAB, (f) PANI-3 obtained from UV-vis spectra by plotting $(F(R_\infty)h\nu)^2$ versus $h\nu$ and $(F(R_\infty)h\nu)^{1/2}$ versus $h\nu$ respectively.